Snow Melt Onset Over Arctic Sea Ice from SMMR and SSM/I-SSMIS Brightness Temperatures, Version 3

USER GUIDE

How to Cite These Data

As a condition of using these data, you must include a citation:

Anderson, M., A. C. Bliss, and S. Drobot. 2014. *Snow Melt Onset Over Arctic Sea Ice from SMMR and SSM/I-SSMIS Brightness Temperatures, Version 3* [Indicate subset used]. Boulder, Colorado USA. NASA National Snow and Ice Data Center Distributed Active Archive Center. https://doi.org/10.5067/22NFZL42RMUO. [Date Accessed].

FOR QUESTIONS ABOUT THESE DATA, CONTACT NSIDC@NSIDC.ORG

FOR CURRENT INFORMATION, VISIT https://nsidc.org/data/NSIDC-0105

National Snow and Ice Data Center

TABLE OF CONTENTS

1 DETAILED DATA DESCRIPTION

This data set includes yearly snow melt onset dates over Arctic sea ice derived from brightness temperatures from the Scanning Multichannel Microwave Radiometer (SMMR), the Special Sensor Microwave/Imager (SSM/I), and the Special Sensor Microwave Imager/Sounder (SSMIS). The introduction of liquid water to snow results in a sharp increase in the emissivity and hence brightness temperature of the snowpack. Snow melt onset is defined as the point in time when microwave brightness temperatures increase sharply due to the presence of liquid water in the snowpack. Data span the years 1979 through 2012 and are in a polar stereographic grid at 25 km resolution. Flat binary, 1-byte integer files and GIF images are accessible via FTP. Several value-added products are also available in flat binary, 4-byte floating point files.

Value-added data sets include the following for each pixel: mean melt onset date, latest (maximum) melt onset date, earliest (minimum) melt onset date, range of melt onset dates (the difference between maximum and minimum -- an index of variability), and standard deviation of melt onset date (another index of variability). Graphical representations of value-added data are also available.

1.1 Format and File Description

1.1.1 Data Files and Browse Image Files

Data are in flat binary format, in 304 by 448 pixel grids. A GIF-formatted graphical representation of each data file is also available. Data fields are 1-byte integers with values ranging from 0 to 245

1.1.2 Ancillary, Value-Added Files

Statistics provided in these files are calculated over the 1979-2012 time period for each pixel. Values in the ancillary files below are calculated only for pixel locations where a melt onset date was calculated for all 34 years of the data record. The fields of the binary (.bin) data files are 4-byte floating point numbers and the browse images (.gif) show a graphical representation of the binary data files. Table 1 describes each file.

Table 1. Ancillary, Value-Added Files Description

Parameter (unit)	Data File Name (Browse Image Name)	Description
Mean (DOY)	melt_mean_1979-2012_v3_n.bin (melt_mean_1979-2012_v3_n.gif)	Mean melt onset date (1979-2012)
Median (DOY)	melt_median_1979-2012_v3_n.bin (melt_median_1979-2012_v3_n.gif)	Median melt onset date (1979-2012)
Latest (DOY)	melt_latest_1979-2012_v3_n.bin (melt_latest_1979-2012_v3_n.gif)	Latest (maximum) melt onset date observed over the climatology
Earliest (DOY)	melt_earliest_1979-2012_v3_n.bin (melt_earliest_1979-2012_v3_n.gif)	Earliest (minimum) melt onset date observed over the climatology
Range (days)	melt_range_1979-2012_v3_n.bin (melt_range_1979-2012_v3_n.gif)	Latest minus earliest melt onset date
Standard Deviation (days)	melt_stdev_1979-2012_v3_n.bin (melt_stdev_1979-2012_v3_n.gif)	Standard deviation in melt onset

1.1.3 File and Directory Structure

Each melt onset data file represents one year of data. The time series is comprised of 34 flat binary files and 34 GIF images. The files range in size from 26 KB to 32 KB for a total data set volume of approximately 2.2 MB.

1.2 File Naming Convention

1.2.1 Data Files and Browse Image Files

The file naming convention for the data files and the browse image files is the following and as described in Table 2.

```
melt_YYYY_vVV_n.ext
```

Where:

Table 2. File Naming Convention Values

Variable	Description
melt	Indicates the file contains snow melt onset
yyyy	4-digit year
n	Hemisphere (n: Northern)
vVV	Version (v03)
.ext	File extension: .bin = binary, .gif = GIF browse image

Example:

```
melt_2007_v03_n.bin
```

1.2.2 Ancillary, Value-Added Files

Ancillary, value-added files are named according to the following convention and as described in Table 3.

```
melt_parameter_1979-YYYY_v03_n.ext
```

Where:

Table 3. File Naming Convention Values

Variable	Description
melt	Snow melt onset
parameter	Valid parameter values: earliest, latest, mean, median, range, and stdev
1979-yyyy	Temporal coverage: 1979 through 4-digit year
n	Hemisphere (n: Northern)
vVV	Version (v03)
.ext	File extension: .bin = binary, .gif = GIF browse image

Example:

```
melt_median_1979-2012_v03_n.gif
```

1.3 Spatial Coverage and Resolution

Data cover the Northern Hemisphere, except for circular sectors centered over the pole. Data from the SMMR period (1978-87) have a polar gap 611 km in radius, located poleward of 84.5 degrees North latitude. Data from the SSM/I period (1987 through 2007) and the SSMIS period (2008 through 2012) have a polar gap 311 km in radius, located poleward of 87.2 degrees North latitude.

See the Polar Stereographic Projection and Grid spatial coverage map for details. Spatial resolution is 25 km for all sensors.

1.3.1 Projection

Data are in a polar stereographic projection with a plane of tangency at 70 degrees north latitude. For a complete description, see the Polar Stereographic Projection and Grid web page.

1.3.2 Grid Description

Grids are the same as those of the DMSP SSM/I-SSMIS Daily Polar Gridded Brightness Temperatures; however, only the Northern Hemisphere grid is used in this data set. The grid cell resolution is 25 km true at 70 degrees north latitude. Grid orientation is such that the first data value for the Northern Hemisphere corresponds to 30.98 degrees latitude and 168.35 degrees longitude. The origin of each x, y grid is the pole.

The grids' approximate outer boundaries are defined by corner points in Table 4. Apply values to the polar grids reading clockwise from upper left. Interim rows define boundary midpoints.

Table 4. Northern Hemisphere Polar Stereographic Grid Coordinates

X (km)	Y (km)	Latitude (deg)	Longitude (deg)	Position in Pixel
-3850	5850	30.98	168.35	corner
0	5850	39.43	135.00	midpoint
3750	5850	31.37	102.34	corner
3750	0	56.35	45.00	midpoint
3750	-5350	34.35	350.03	corner
0	-5350	43.28	315.00	midpoint
-5850	-5350	33.92	279.26	corner
-5850	0	55.50	225.00	midpoint

1.4 Temporal Coverage and Resolution

Snow melt onset data range from 1979 through 2012, as shown in Table 5. Data are derived from brightness temperatures acquired from multiple platforms. Snow melt onset data are derived once per year for each grid cell.

Note: Only brightness temperatures for DOY 61 through 245 are used.

Table 5. Temporal Coverage

Data Type/Sensor	Start Date	End Date
Nimbus-7 SMMR	1 Jan 1979	20 August 1987[1]
DMSP F8 SSM/I	1 Jan 1988	18 December 1991
DMSP F11 SSM/I	1 Jan 1992	31 December 1995
DMSP F13 SSM/I	1 Jan 1996	31 December 2007
DMSP F17 SSMIS	1 Jan 2008	31 December 2012
[1]For the last 11 days of the melt season for August 1987, F8 data is not substituted for the missing SMMR days. Those dasys are treated as having no data and do not calculate a melt onset date.		

1.5 Parameter or Variable

1.5.1 Parameter Description

Each pixel represents the day of the year that melt first began. The introduction of liquid water to snow results in a sharp increase in the emissivity and hence brightness temperature of the snowpack. Snow melt onset is defined as the point in time when microwave brightness temperatures increase sharply due to the presence of liquid water in the snowpack.

See the 3.3 section of this document for information regarding derivation of snow melt onset values.

1.5.2 Parameter Range

Table 6. Parameter Values and Description

Value	Description
0	Indicates that no melt date was calculated and also includes locations where there is open ocean, land, the pole hole, or locations within the sea ice pack where no melt onset occurred for that year.
61-245	Day of melt onset (units: DOY)

Sample Browse Image

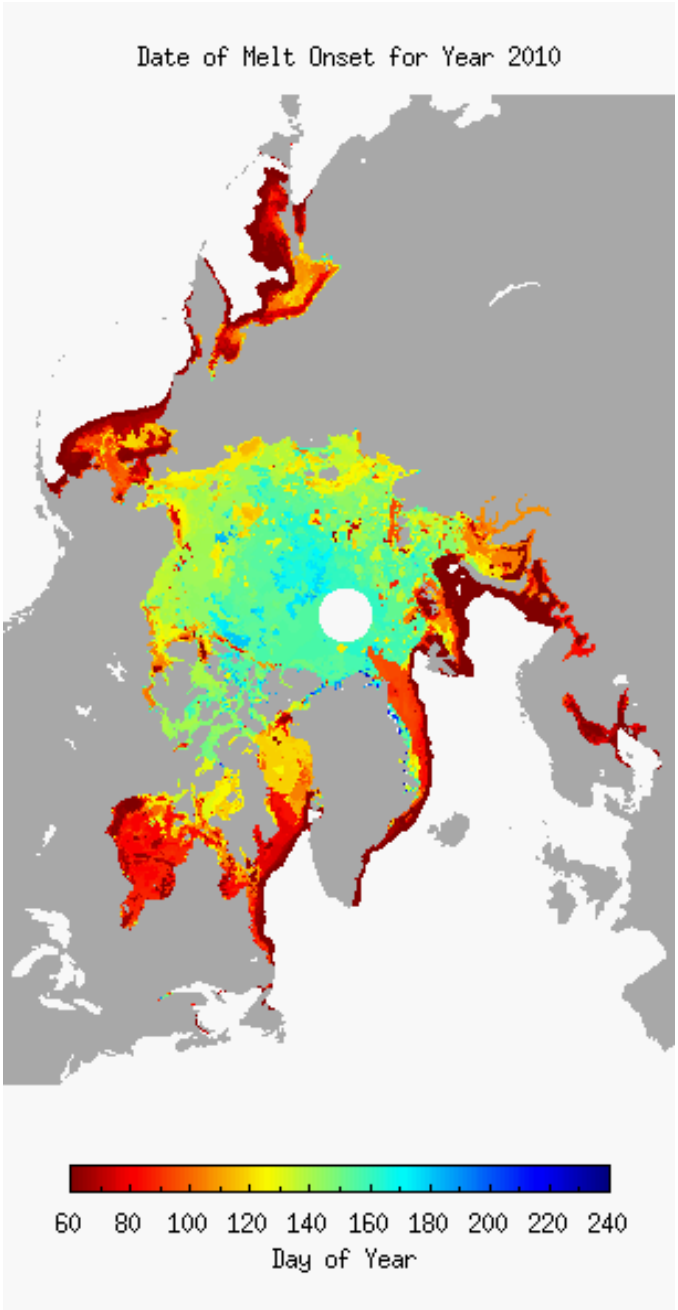

Figure 1. Browse Image for 2010 v3 Data

1.6 Applications

Accurate dates of snow melt onset over sea ice contribute to improved simulations of climate during the Arctic snow melt period. Records of the spatial and temporal variability in snow melt can serve as climate proxies in Arctic sea ice zones (Drobot and Anderson 2001b).

Snow melt onset affects the Arctic energy balance as surface albedo decreases and energy absorption increases in response to the appearance of liquid water (Drobot and Anderson 2001b). Initial locations of sea ice melt vary both spatially and temporally. Melt signatures appear first in lower latitudes and advance northward with time. Along the Asian Arctic coast, snow melt starts in the far eastern (Chukchi Sea) and western (Barents and Kara Seas) regions. Over several weeks, the melt progresses zonally toward the Laptev Sea (Anderson 1987).

1.7 Error Sources

Brightness temperature data may introduce errors related to pixel averaging, sensor errors, and weather effects. See the following temperature documentation for more information regarding errors in the source data:

- DMSP SSM/I-SSMIS Daily Polar Gridded Brightness Temperatures
- Nimbus-7 SMMR Polar Radiances and Arctic and Antarctic Sea Ice Concentrations

1.7.1 Limitations of the Data

Given the short data record and the known errors, users are advised against selecting individual pixels without examining surrounding data points. Also, trend analysis at any given pixel should include a study of nearby pixels to confirm that results are locally consistent.

2 SOFTWARE AND TOOLS

For a comprehensive list of all polar stereographic tools and for more information, see the Polar Stereographic Data Tools Web page.

3 DATA ACQUISITION AND PROCESSING

3.1 Theory of Measurements

Microwave emmissivity of snow increases dramatically as the snow melts and liquid water appears. With the presence of liquid water in the snow pack, surface scattering dominates over volume scattering, resulting in a sharp increase in the brightness temperatures signature. Lower microwave frequencies (19.3 GHz for the SSM/I instrument and 18.0 GHz for the SMMR instrument) are more responsive to melt onset in the firn than are higher frequencies (37.0 GHz for both SSM/I and SMMR), due primarily to the change in emission depth associated with melt. This causes the difference between 19.3 (or 18.0) GHz and 37.0 GHz brightness temperatures to change from positive to near-zero or negative (Kunzi et al. 1982). Furthermore, the increase in brightness temperature associated with melt is frequency- and polarization-dependent. Horizontal channels reflect a stronger dependence on snow conditions during melt (Anderson 1997) due to the change in dielectric properties at the air-snow interface when snow is wet (Abdalati and Steffen 1995).

3.2 Data Acquisition Methods

Brightness temperature data were acquired by the SMMR, SSM/I, and SSMIS instruments. Table 7 provides a specific list of the data sets used and the channels from the instruments.

Table 7. Input Data Sets

Data Set	Description	Channels/Variables Used
Nimbus-7 SMMR Polar Gridded Radiances and Sea Ice Concentrations (Gloersen 1994)	Brightness temperatures used to calculate snow melt onset dates (1979-1987)	18GHz and 37GHz
DMSP SSM/I-SSMIS Daily Polar Gridded Brightness Temperatures, Version 4 (Maslanik and Stroeve 2012)	Brightness temperatures used to calculate snow melt onset dates (1988-2012)	19GHz and 37GHz
NOAA/NSIDC Climate Data Record of Passive Microwave Sea Ice Concentration, Version 2 (Meier et al. 2013)	Sea ice concentrations used to create mask of annual sea ice maximum extent. Melt dates calculated for locations in sea ice mask.	goddard_merged_seaice_conc

3.3 Derivation Techniques and Algorithms

Drobot and Anderson calculate snow melt onset dates using daily-averaged brightness temperature data from SMMR, SSM/I (F8, F11, and F13), and SSMIS (F17) satellite radiometers. See Table 7 for a complete list of input data. The investigators record changes in 19H GHz and 37H GHz brightness temperatures for each data point on each day within a 20-day window using the Advanced Horizontal Range Algorithm (AHRA) (Anderson 1997).

3.3.1 Version History

Table 8 outlines the processing and algorithm history for this product.

Table 8. Description of Version Changes

Version	Date	Description of Changes from Previous Version
V03	Mar 2014	Updates the data record to span through the 2012 melt season which includes the use of the SSMIS instrument on the DMSP F17 satellite. The two-pixel buffer surrounding the coastlines has been removed. Included the use of an annual sea ice extent mask to indicate sea ice locations where a melt onset date is calculated. Changed the regression coefficients used to convert the F11 brightness temperatures to use ones from the Northern Hemisphere sea ice overlap area of Stroeve et al. (1998). Parameter values changed from 0 to 255 (inclusive) to 0 to 245 (inclusive). See Table 6 for a description of the parameter values for v3. Trend files are no longer being generated for v3. The gsfc_25n.msk land/coast mask is used.
V02	Nov 2009	Removed 9-point median filter that corrected for spurious melt dates in V01 Added flags in input brightness temperatures to correct for bad scanlines, then reprocessed input brightness temperatures Updated data and documentation to reflect change to V02
V01	Dec 2001	Original version of data.

3.3.2 Version 3 Processing Steps

1. To ensure a consistent data set, SSM/I F8 is used as the standard sensor and regression analysis was used to convert SMMR, SSM/I F11 and F13, and SSMIS F17 brightness temperatures to SSM/I F8 brightness temperatures during overlap periods (after Abdalati et al. 1995). Table 9 provides an overview of the correction coefficients used. This ensures a consistent data record for determining temporal trends in the snow melt onset dates. If data are not consistent, snow melt trends could be attributed to instrument characteristics rather than climate conditions. The following conversions were made to create a consistent data set:
    - Converted SMMR brightness temperatures to SSM/I F8 brightness temperatures using slope and intercept values from Jezek et al. (1991).
    - Converted SSM/I F11 brightness temperatures to SSM/I F8 brightness temperatures using slope and intercept values from Abdalati et al. (1995).
    - Converted SSM/I F13 brightness temperatures to SSM/I F11 brightness temperatures using slope and intercept values from the Northern Hemisphere sea ice overlap area from Stroeve et al. (1998).
    - Converted SSMIS F17 brightness temperatures to SSM/I F13 brightness temperatures using slope and intercept values from W. Meier (personal communication Oct. 2011).
2. Determine which pixels have a sea ice concentration ≥ 50% on one or both of the first two days with sea ice concentration data beginning on day of year (DOY) 61. A melt onset date is calculated only at pixel locations that meet this criterion.

- The goddard_merged_seaice_conc variable from the NOAA/NSIDC Climate Data Record of Passive Microwave Sea Ice Concentration, Version 2 data set is used for the daily sea ice concentration.
- DOY 61 (at the beginning of March) is used because this date roughly corresponds to the time period of maximum annual sea ice extent.
- In the event of data outages (i.e. a missing swath), sea ice concentrations of 50% or greater on one or both of the first two days are used. Note that SMMR data were collected every other day, so the first two days with data between DOY 61 and DOY 65 may be used to define the sea ice area.

3. Used an annual sea ice mask for each year created using the sea ice extent (where concentration is 50%) at the beginning of March to remove pixels that would not have melt calculated. This differs from version 2 that used a climatology mask to remove pixels where the melt date was not calculated.
4. Implemented the melt algorithm (AHRA) as described in Drobot and Anderson (2001b).
   - If the difference between 19H GHz and 37H GHz is greater than 4 K at a given point, the AHRA assumes winter conditions and proceeds to the next day for that point.
   - If the difference between 19H GHz and 37H GHz is -10 K or less, then the AHRA assumes liquid water is present in the snowpack and classifies that day as the snow melt onset date.
   - If the difference between 19H GHz and 37H GHz is less than 4 K but greater than -10 K, the AHRA determines if snow melt onset occurred based on a 20-day time series of brightness temperatures. The algorithm subtracts the minimum and maximum values for the ten days prior to the potential melt onset date, and again for the period from the potential melt onset date to nine days later. The former number is subtracted from the latter number. If the difference is greater than 7.5 K, the algorithm assigns melt to that particular pixel. A large difference indicates variability in the 19H - 37H range after the potential melt onset date. If the difference is less than 7.5 K, then liquid water is unlikely to be in the snowpack, and the algorithm moves on to the next day (Drobot and Anderson 2001b).
5. Assigned a value of 0 to all pixels that were open ocean, land, part of the polar gap, or if melt was not calculated at that location.

Table 9. Linear Regression Coefficients and Equations Used to Calibrate TBs Between SMMR, SSMI, and SSMIS Sensors using F8 as the Standard

Sensor Correction	Source	Overlap Area	Channels	Coefficients		Correction Equation
SMMR to F8	Jezek et al. (1991)	---	18H	Slope	0.940	F8=(SMMR-2.62)/0.940
				Int. (K)	2.62	
			37H	Slope	0.954	F8=(SMMR-2.85)/0.954
				Int. (K)	2.85	
F11 to F8	Abdalati et al. (1995)	Greenland	19H	Slope	1.013	F8=1.013*F11-1.890
				Int. (K)	-1.89	
			37H	Slope	1.024	F8=1.024*F11-4.220
				Int. (K)	-4.22	
F13 to F11	Stroeve et al. (1998)	NH Sea Ice	19H	Slope	0.986	F11=(F13-2.197)/0.986
				Int. (K)	2.179	
			37H	Slope	0.966	F11=(F13-6.110)/0.966
				Int. (K)	6.11	
F17 to F13	Walt Meier (Personal Communication Oct. 2011)	Arctic Mar-Sept 2007	19H	Slope	0.979	F13=(F17-1.646)/0.979
				Int. (K)	1.646	
			37H	Slope	0.999	F13=(F17-0.649)/0.999
				Int. (K)	0.649	

3.4 Sensor or Instrument Description

For details regarding instruments and platforms, refer to the SMMR, SSM/I, and SSMIS Sensors Summary.

4 REFERENCES AND RELATED PUBLICATIONS

Abdalati, W. and K. Steffen. 1997. Snowmelt on the Greenland Ice Sheet as Derived from Passive Microwave Satellite Data. *Journal of Climate* 10(2):165-175.

Abdalati, W. and K. Steffen. 1995. Passive Microwave-defined Snow Melt Regions on the Greenland Ice Sheet. *Geophysical Research Letters* 22(7):787-790.

Abdalati, W., K. Steffen, C. Otto and K. Jezek. 1995. Comparison of brightness temperatures from SSM/I Instruments on the DMSP F8 and F11 Satellites for Antarctica and the Greenland Ice Sheet. *International Journal of Remote Sensing* 16:1223-1229.

Anderson, M. 1997. Determination of a Melt Onset Date for Arctic Sea Ice Regions Using Passive Microwave Data. *Annals of Glaciology* 25:382-387.

Anderson, M. 1987. The Onset of Spring Melt in First-year Ice Regions of the Arctic as Determined from Scanning Multichannel Microwave Radiometer Data for 1979 and 1980. *Journal of Geophysical Research* 92(C12):13,153-13,163.

Cavalieri, D., C. Parkinson, P. Gloersen, J. Comiso, and H. J. Zwally. 1999. Deriving Long-term Time Series of Sea Ice Cover from Satellite Passive-microwave Multisensor Data Sets. *Journal of Geophysical Research* 104(C7):15,803-15,814.

Cavalieri, D. 1994. A Microwave Technique for Mapping Thin Sea Ice. *Journal of Geophysical Research* 99(C6):12,561-12,572.

Drobot, S. D. and M. R. Anderson. 2001a. An improved method for determining snowmelt onset dates over Arctic sea ice using scanning multichannel microwave radiometer and Special Sensor Microwave/Imager data. *Journal of Geophysical Research* 106: 24,033-24,049.

Drobot, S. and M. Anderson. 2001b. Comparison of Interannual Snowmelt Onset Dates with Atmospheric Conditions. *Annals of Glaciology* 33: 79-84.

Dubach L. and C. Ng. 1988. NSSDC's Compendium of Meteorological Space Programs, Satellites, and Experiments.

Gloersen, P. 1994. Nimbus-7 SMMR Polar Radiances and Arctic and Antarctic Sea Ice Concentrations. [1979-1987]. Boulder, Colorado USA: National Snow and Ice Data Center.

Gloersen, P. and F. Barath. 1977. A Scanning Multichannel Microwave Radiometer for Nimbus-G and SeaSat-A. *IEEE Journal of Oceanic Engineering* 2:172-178.

Gloersen, P., W. Campbell, D. Cavalieri, J. Comiso, C. Parkinson, and H. J. Zwally. 1992. Arctic and Antarctic Sea Ice, 1978-1987: *Satellite Passive-microwave Observations and Analysis.* National Aeronautics and Space Administration Scientific and Technical Information Program. Washington, D.C.

Gloersen, P. and L. Hardis. 1978. The Scanning Multichannel Microwave Radiometer (SMMR) Experiment, in *The Nimbus 7 Users' Guide.* C. R. Madrid, editor. National Aeronautics and Space Administration. Greenbelt, MD: Goddard Space Flight Center.

Jezek, K., C. Merry, D. Cavalieri, S., Grace, J. Bedner, D. Wilson, and D. Lampkin. 1991. Comparison Between SMMR and SSM/I Passive Microwave Data Collected over the Antarctic Ice

Sheet. Byrd Polar Research Center Technical Report No. 91-03, The Ohio State University, Columbus, Ohio, 62 pp.

Kramer, H. 1994. *Observation of the Earth and Its Environment* - Survey of Missions and Sensors, 2nd Edition. Heidelberg: Springer-Verlag.

Kunzi, K., S. Patil, and H. Rott. 1982. Snow-cover Parameters Derived from Nimbus-7 Scanning Multichannel Microwave Radiometer (SMMR) data. *IEEE Transactions on Geosciences and Remote Sensing* GE-20:57-66.

Livingstone, C., K. Singh, and L. Gray. 1987. Seasonal and Regional Variations of Active/Passive Microwave Signatures of Sea Ice. *IEEE Transactions on Geosciences and Remote Sensing* GE-25:159-172.

Maslanik, J. and J. Stroeve. 2004, updated 2012. DMSP SSM/I-SSMIS Daily Polar Gridded Brightness Temperatures. Version 4. [1988-2011]. Boulder, Colorado USA: NASA DAAC at the National Snow and Ice Data Center.

Meier, W., F. Fetterer, M. Savoie, S. Mallory, R. Duerr, and J. Stroeve. 2013. NOAA/NSIDC Climate Data Record of Passive Microwave Sea Ice Concentration. Version 2. [2008-2011]. Boulder, Colorado USA: National Snow and Ice Data Center. http://dx.doi.org/10.7265/N55M63M1.

National Aeronautics and Space Administration. 1978. The Nimbus 7 Users' Guide. C.R. Madrid, editor. Goddard Space Flight Center.

Snyder, J. P. 1982. Map Projections Used by the U.S. Geological Survey. U.S. Geological Survey Bulletin 1532.

Stroeve, J., L. Xiaoming, and J. Maslanik. 1998. An Intercomparison of DMSP F11- and F13-derived Sea Ice Products. *Remote Sensing of the Environment* 64:132-152.

Swanson, P. and A. Riley. 1980. The Seasat Scanning Multichannel Microwave Radiometer (SMMR): Radiometric Calibration Algorithm Development and Performance. *IEEE Journal of Oceanic Engineering* OE-5:116-124.

4.1 Related Data Collections

- MEaSUREs Arctic Sea Ice Characterization Daily 25km EASE-Grid 2.0
- DMSP SSM/I-SSMIS Daily Polar Gridded Brightness Temperatures
- Nimbus-7 SMMR Polar Radiances and Arctic and Antarctic Sea Ice Concentrations
- ESMR Polar Gridded Brightness Temperatures and Sea Ice Concentrations
- Near-Real-Time DMSP SSM/I-SSMIS Daily Polar Gridded Brightness Temperatures

- Near-Real-Time DMSP SSM/I-SSMIS Daily Polar Gridded Sea Ice Concentrations
- DMSP SSM/I-SSMIS Pathfinder Daily EASE-Grid Brightness Temperatures
- Sea Ice Concentrations from Nimbus-7 SMMR and DMSP SSM/I-SSMIS Passive Microwave Data
- Bootstrap Sea Ice Concentrations from Nimbus-7 SMMR and DMSP SSM/I
- Sea Ice Trends and Climatologies from SMMR and SSM/I-SSMIS
- NOAA/NSIDC Climate Data Record of Passive Microwave Sea Ice Concentration, Version 2

5 CONTACTS AND ACKNOWLEDGMENTS

Mark Anderson

Meteorology/Climatology Program

Department of Geosciences

University of Nebraska

Lincoln, NE 68588-0340 USA

Sheldon Drobot

Research Applications Lab

National Center for Atmospheric Research (NCAR)

University Corporation for Atmospheric Research (UCAR)

P.O. Box 3000

Boulder, CO 80307-3000 USA

6 DOCUMENT INFORMATION

6.1 Publication Date

December 2001

6.2 Date Last Updated

March 2014